JOURNAL OF THE KOREAN ASTRONOMICAL SOCIETY
36: 271 ~ 282, 2003

DENSE MOLECULAR CLOUDS IN THE GALACTIC CENTER REGION II. $H^{13}CN$ (J=1-0) DATA AND PHYSICAL PROPERTIES OF THE CLOUDS

CHANG WON LEE[1] AND HYUNG MOK LEE[2]
[1]Korea Astronomy Observatory, 61-1 Hwaam-dong, Yusung-gu, Daejon 305-348, Korea
E-mail: cwl@trao.re.kr
[2]SEES, Seoul National University, Seoul 151-742, Korea
E-mail: hmlee@astro.snu.ac.kr
(Received November 18, 2003; Accepted December 19, 2003)

ABSTRACT

We present results of a $H^{13}CN$ J=1−0 mapping survey of molecular clouds toward the Galactic Center (GC) region of $-1.6° \leq l \leq 2°$ and $-0.23° \leq b \leq 0.30°$ with 2′ grid resolution. The $H^{13}CN$ emissions show similar distribution and velocity structures to those of the $H^{12}CN$ emissions, but are found to better trace the feature saturated with $H^{12}CN$ (1-0). The bright components among multi-components of $H^{12}CN$ line profiles usually appear in the $H^{13}CN$ line while most of the dynamically forbidden, weak $H^{12}CN$ components are seldom detected in the $H^{13}CN$ line.
We also present results of other complementary observations in ^{12}CO (J=1-0) and ^{13}CO (J=1-0) lines to estimate physical quantities of the GC clouds, such as fractional abundance of HCN isotopes and mass of the GC cloud complexes. We confirm that the GC has very rich chemistry. The overall fractional abundance of $H^{12}CN$ and $H^{13}CN$ relative to H_2 in the GC region is found to be significantly higher than those of any other regions, such as star forming region and dark cloud. Especially cloud complexes nearer to the GC tend to have various higher abundance of HCN. Total mass of the HCN molecular clouds within $|l| \leq 6°$ is estimated to be $\sim 2 \times 10^7\,M_\odot$ using the abundances of HCN isotopes, which is fairly consistent with previous other estimates. Masses of four main complexes in the GC range from a few 10^5 to $\sim 10^7\,M_\odot$. All the HCN spectra with multi-components for the four main cloud complexes were investigated to compare the line widths of the complexes. The largest mode (45 km s^{-1}) of the FWHM distributions among the complexes is in the Clump 2. The value of the mode tends to be smaller at the farther complexes from the GC.

Key words : The Galaxy: center - clouds: HCN isotopes: column density: abundance: mass

I. INTRODUCTION

The molecular clouds within a few hundreds parsecs from the Galactic Center (GC) are in very unique environment, being affected by high mass concentration ($\sim$ 10% of the total gas of the Galaxy), strong energetics, tidal force, magnetic fields and so on in the GC (e.g. Güsten 1989, Morris 1996). Such activities in the GC may force the GC clouds to be characterized by high temperature (typically $\sim$ 70 K), very large internal velocity dispersion ($\sim 15-50$ km s^{-1}), high density ($\geq 10^4$ cm^{-3}), and even the rich chemistry (e.g., Lee, Minh, & Irvine 1993).

During the last decade there were many mapping surveys of the GC molecular clouds with various spatial scale of a few tens minutes to a few tens arc-seconds in various molecular lines to improve understanding on the distribution, kinematics, and statistical properties of the GC clouds (Table 1). With a few arc minutes scale, it has been found that the GC clouds are affected by non-axisymmetric 'barred' potential and some of the GC clouds exhibit a peculiar velocity not permitted by the uniform circular rotation of the Galaxy (e.g., Lee 1996 - hereafter paper 1, Lee et al. 1999). The distribution of the GC clouds is heavily lopsided to the first quadrant (e.g., Bally et al. 1988, paper 1). Recent trend in the observational study of the GC clouds is to conduct high angular resolution observations to study detailed properties of individual GC clouds in 1 ~ 2 pc scale. For example, using CS(1-0) data of 30″ resolution, Miyazaki & Tsuboi (2000) identified $\sim$ 160 clouds and found that the GC molecular clouds have very similar mass and size spectra to those in the Galactic disk while the line widths of the GC clouds are about 5 times larger than those in the Galactic disk clouds. Oka et al. (2001) used their CO(1-0) data of 34″ grid resolution to identify 165 clouds. They found that relations between the size and line widths, and between virial mass and CO luminosity are similar to those of the Galactic disk.

Apart from the high angular resolution survey, it is also important to make a survey with a very optically thin molecular line. Our previous HCN J=1-0 survey of the GC molecular clouds within $-6° \leq l \leq 6°$ and $-0°.8 \leq b \leq 0°.87$ (paper 1) was very successful to study the kinematics and the distribution of the high

Corresponding Author: C. W. Lee

Table 1. MOLECULAR LINE SURVEYS TOWARD THE GALACTIC CENTER

Molecule	Freq.(GHz)	Longitude	Latitude	Map Grid ($l \times b$)	Beam	Ref.
OH	1.665	$-6°.0 \leq l \leq 8°.6$	$-1°.0 \leq b \leq 1°.0$	$10' \times 12'$	$3.0'$	(1)
^{12}CO	115.271	$-5°.0 \leq l \leq 122°.0$	$-1°.0 \leq b \leq 1°.0$	$3'$	$1.7'$	(2)
^{13}CO	110.201	$-2°.0 \leq l \leq 2°.0$	$-0°.5 \leq b \leq 0°.5$	$4' \times 8'$	$1.7'$	(3)
^{13}CO	110.201	$-5°.0 \leq l \leq 5°.0$	$-0°.6 \leq b \leq 0°.6$	$6'$	$1.7'$	(4)
CS	97.981	$-1°.0 \leq l \leq 3°.7$	$-0°.4 \leq b \leq 0°.4$	$2'$	$1.9'$	(4)
H_2CO	4.830	$0°.5 \leq l \leq 4°.0$	$-0°.5 \leq b \leq 0°.9$	$6'$	$2.9'$	(5)
HCN	88.631	$-6°.0 \leq l \leq 6°.0$	$-0°.8 \leq b \leq 0°.87$	$4'$	$1'$	(6)
^{12}CO	115.271	$-1°.7 \leq l \leq 3°.4$	$-0°.6 \leq b \leq 0°.6$	$34''$	$17''$	(7)
CS	48.991	$-1°.0 \leq l \leq 1°.42$	$-0°.42 \leq b \leq 0°.42$	$30''$	$34''$	(8)
H^{13}CN	86.340	$-1°.6 \leq l \leq 2°.0$	$-0°.23 \leq b \leq 0°.30$	$2'$	$1'$	this study

REFERENCES.— (1) Cohen & Dent 1983; (2) Stark *et al.* 1988; (3) Heiligman 1987; (4) Bally *et al.* 1987; (5) Zylka *et al.* 1992; (6) Lee 1996; (7) Oka et al. 1998; (8) Miyazaki & Tsuboi 2000.

density clouds in the GC. However, HCN (1-0) line itself is also found to be severely saturated in several GC clouds especially near to the GC, making hard to see detailed distribution and velocity structure of the clouds. This case requires observations with optically thinner isotope tracer like H^{13}CN(1-0) to look at more details of velocity structure and gas distribution of the clouds, with better contrast. In this paper we present the results of the H^{13}CN J=1−0 survey toward the GC clouds within $|l| \leq 2°$ on a grid resolution of $2'$. In addition these data are also useful for deriving their physical quantities such as fractional abundance and mass of the clouds, if other CO observations are combined with the data. So we also present our complementary observations with ^{12}CO J=1-0 line (115.3 GHz) and ^{13}CO J=1-0 to derive the physical quantities of the GC clouds and discuss their physical properties.

This paper is organized as follows. The observational procedure and data reduction are described in §2. In §3 the data of H^{13}CN (1-0) are presented in the form of various maps. In §4 the physical quantities of the GC clouds are derived and discussed. In the last section a summary of this paper is given.

II. OBSERVATIONS AND DATA REDUCTIONS

A survey of the H^{13}CN J=1−0 transition (ν = 86.340184 GHz) was carried out toward the GC region of $-1.6° \leq l \leq 2°$ and $-0.23° \leq b \leq 0.30°$ on a grid resolution of $2'$. The total number of observed spectra is $\sim$ 1050. Several sample spectra from the survey regions are shown in Fig. 1-(a) together with H^{12}CN J=1−0 spectra.

Complementary observations of ^{12}CO (J=1-0) line and ^{13}CO (J=1-0) line, which are necessary to derive the column density of N(H_2), were also made on the region of $|l| \leq 2°$ on a $4'$ spacing along Galactic longitude at $b = -4'$. Several other positions ($|l| > 2°$) which show strong emissions in H^{12}CN 88.6GHz are also observed with CO lines. Sample spectra of all molecular lines obtained at the position of $(l, b) = (0°, -0.0667°)$ are shown in Fig. 1-(b).

Observations were all made with the 14 m telescope of the Taeduk Radio Astronomy Observatory (TRAO) in Korea. Observational parameters for TRAO telescope in observations are summarized in Table 2.

Spectral line intensities were calibrated and corrected for atmospheric losses using chopper wheel method to obtain the antenna temperature T_A^*. Most of the data were taken with a position switching mode. Reference positions for CO observations were chosen on the emission free regions of $b \approx 2° \sim 3°$ and reference positions for H^{13}CN observations on the regions of $b \approx 1°$. The pointing accuracy of the telescope was usually better than $\sim 20''$. The data reductions were made with the DOS-version of the FCRAO SPA software that the TRAO has modified, and NRAO AIPS software.

III. THE H^{13}CN DATA

(a) Total Velocity Integrated Map

Total velocity integrated intensity map of H^{13}CN J=1-0 line is given in Fig. 2-(a), where the map of H^{12}CN J=1-0 line is also shown in Fig. 2-(b) for the comparison between two maps. The figure shows that the distribution of H^{13}CN emissions is similar to that of strong H^{12}CN J=1-0 emissions, except that the H^{13}CN map shows more clumpy structures due to its higher grid mapping resolution and less severe saturation than the H^{12}CN map. The distribution of H^{13}CN emission lopsided at the positive longitude is similar to that of the H^{12}CN emission cores. Prominent features are Sgr A, B, C, D, and $l \approx 1.3°$ complexes. It is noted that

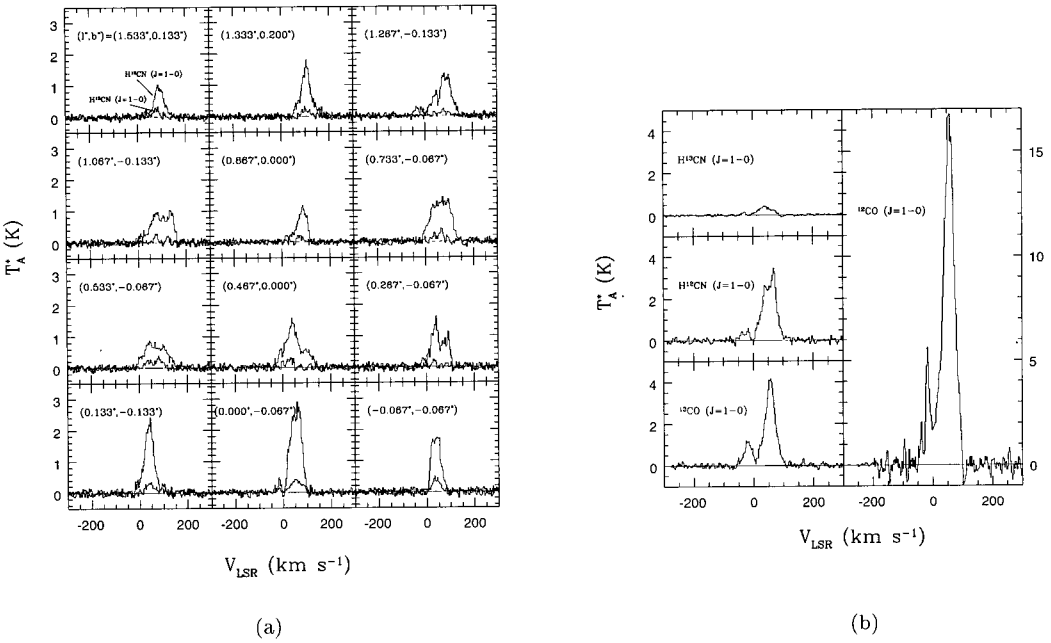

Fig. 1.— (a) Sample spectra of $H^{12}CN$ (J=1-0) and (b) sample spectra of $H^{12}CN$ (J=1-0), $H^{13}CN$ (J=1-0), ^{12}CO (J=1-0), and ^{13}CO (J=1-0) lines taken at $(l, b) = (0°, -0.0667°)$.

the strongest emitting line comes from the Sgr B region while the strongest $H^{12}CN$ J=1-0 line comes from the Sgr A.

(b) Velocity Channel Maps

We present two channel maps: one binned into 100 km s^{-1} intervals (Fig. 3) and the other binned into 20 km s^{-1} intervals (Fig. 4). Unlike the $H^{12}CN$ maps, the maps show relatively simple velocity structures. This is because the weak wing parts and forbidden components seen at the $H^{12}CN$ line barely appeared in the $H^{13}CN$ line and thus only the strong components among multi-components of $H^{12}CN$ line profiles tend to appear in the $H^{13}CN$ line. Therefore the velocity range is mostly limited within $|V_{LSR}| \leq 100$ km s^{-1}. This velocity structure of the line emissions is also similar to that of the cores of $H^{12}CN$ emissions.

Most of emissions have velocities permitted by Galactic rotation except for Sgr A clouds between $l \approx -0.3° \sim 0°$ which have positive velocity components of $0 \sim 80$ km s^{-1} at the negative longitude.

(c) Space - Velocity Maps

We present the $l - V$ diagram averaged over b (Fig. 5) and $l - V$ diagrams at several latitude b (Fig. 6). These maps also confirm that the $H^{13}CN$ map traces core structures shown at the $H^{12}CN$ map (Fig. 6 of paper 1). The lopsided distribution of the $H^{13}CN$ emissions at the positive longitude is similar to that of cloud cores seen in $H^{12}CN$.

Moreover the $H^{13}CN$ map shows the velocity structures of the saturated region of the HCN clouds in the GC with somewhat better contrast. For example, the velocity structures of emission features shown at the $l - V$ diagram at $b = -4'$ of the Fig. 6, which are indeed hard to see in the saturated $H^{12}CN$ map, are very interesting: The Sgr A and B emission cores have very large velocity gradients of about 2.1 and 5.2 km s^{-1} pc^{-1} at Sgr A and B, respectively, comparing with ~ 0.7 km s^{-1} pc^{-1} for the velocity gradients inferred from the Galactic rotation within ~ 350 pc.

IV. PHYSICAL QUANTITIES OF THE GC CLOUDS

(a) Abundance of HCN Isotopes

The fractional abundance of HCN isotopes relative to H_2 can be estimated when the column density of H_2–$N(H_2)$, and the column density of HCN isotopes are obtained. Here we introduce the methods to derive column densities of each tracers and the abundance of the HCN isotopes.

i) Column Density of ^{13}CO and H_2

$N(H_2)$ is usually obtained from derivation of ^{13}CO column density $N(^{13}CO)$ as described below.

The method needs ^{12}CO and ^{13}CO data. $N(^{13}CO)$ can be derived by the LTE method outlined by Dickman (1978) if the following assumptions are valid:

Table 2. OBSERVATIONAL PARAMETERS OF TELESCOPE SYSTEM

Contents	115.3 GHz	110.2 GHz	88.6 GHz	86.3 GHz
HPBW[a]	$52.3''$	$52.3''$	$61''$	$61''$
η_B^a	0.44	0.44	0.41	0.41
Receiver	S[b]	S	S	SIS[c]
Filter bank	1 MHz×256	1 MHz×256	1 MHz×256	1 MHz×256
Dates of observation	March 1995	Oct. 1995	Oct. 1993 - May 1994	March-May 1995
Filter bank	1 MHz×256	1 MHz×256	1 MHz×256	1 MHz×256
T_{sys}	$1500 \sim 1900$	$800 \sim 1100$	$500 \sim 600$	$600 \sim 800$
T_{int}^d	$2^m \sim 5^m$	$3^m \sim 4^m$	$2^m \sim 3^m$	$4^m \sim 6^m$
T_{rms}	$0.2 \sim 0.8$	$0.09 \sim 0.2$	$0.06 \sim 0.09$	$0.05 \sim 0.08$

REFERENCES.—[a] η_B is main beam efficiency. The numeric values are from Park *et al.* (1994). [b] Schottky diode mixer type. [c] SIS mixer type.[d] Integration time on source.

(1) All molecules along the line of sight lie under the uniform excitation temperature in the J=1-0 transition, (2) the ^{12}CO and ^{13}CO molecules have the same excitation temperature, (3) ^{12}CO J=1-0 line is optically thick, and (4) excitation temperatures for different rotational levels are the same, *i.e.*, , $T_{ex}(J)$ does not depend on the rotational quantum number J.

Under these assumptions, the ^{13}CO column density is given by

$$N(^{13}\mathrm{CO}) = 2.42 \times 10^{14} \frac{T_{ex}\Delta V \tau^{13}}{1 - \exp(-5.289/T_{ex})} \ \mathrm{cm}^{-2}, \quad (1)$$

where ΔV is the FWHM [km s^{-1}], τ^{13} is the optical depth of ^{13}CO J=1-0 line, and T_{ex} is the excitation temperature. The optical depth and the excitation temperature of ^{13}CO can be obtained from the following equation,

$$\tau^{13} = -\ln\left\{1 - \frac{T_A^{*13}}{5.289\eta_B}\left[\frac{1}{\exp(5.289/T_{ex}) - 1} - \frac{1}{\exp(5.289/T_{bg}) - 1}\right]^{-1}\right\}, \quad (2)$$

$$T_{ex} = \frac{5.532}{\ln\left[1 + \frac{5.532}{\frac{T_A^{*12}}{\eta_B} + \frac{5.532}{\exp(5.532/T_{bg}) - 1}}\right]}, \quad (3)$$

where T_A^{*12} and T_A^{*13} are antenna temperatures for ^{12}CO and ^{13}CO lines, respectively, η_B (=0.44) is the main beam efficiency, and T_{bg} is the temperature of the background radiation. In most case no background radiation other than cosmic background is expected and thus T_{bg} can be assumed to be 2.7 K. However, for Sgr A which is known to have the background radio source, as Minh *et al.* (1992) suggested, we assume T_{bg} = 10 K.

Using the observed T_A^{*12} with the assumed T_{bg}, we estimate T_{ex}, which is used to calculate τ^{13}, by equations (2) and (3). The FWHM for each component is obtained from the Gaussian decomposition of the given spectra. Substitution of ΔV together with T_{ex} and τ^{13} to equation (1) enables us to compute $N(^{13}\mathrm{CO})$. From these procedures we derive total ^{13}CO column densities of $2.0 \times 10^{16} \sim 1.2 \times 10^{18}$cm^{-2} for the GC directions as listed in Table 3. By applying the conversion factor of $[^{12}\mathrm{CO}]/[\mathrm{H_2}] = 6 \times 10^{-5}$ (Gordon & Burton 1976) and $[^{12}\mathrm{CO}]/[^{13}\mathrm{CO}] = 27.8$ in the GC (Wannier 1989), we obtain H_2 column densities of $9.0 \times 10^{21} \sim 5.4 \times 10^{23}$ cm^{-2}. The calculated column densities at each observed position are listed in Table 3.

ii) Column Densities of HCN Isotopes [N(HCN) and N(H^{13}CN)]

The column density of a molecular constituent observed in emission is best determined when its optical depth is very small. The optical depth of H^{12}CN (J=1-0) line is estimated to lie between $0.1 \sim 0.6$ if T_{ex} = 20 K is assumed. The optical depth estimates sensitively depends on T_{ex}. The lower values for T_{ex} give higher optical depths. Furthermore, our optical depths would be beam diluted values if the high density clumps are significantly smaller than the beam size of the telescope. Thus the derivation of H^{12}CN column density based on the optically thin assumption of the cloud could give significantly wrong results. In order to avoid such a difficulty, we use the significantly weaker line, H^{13}CN (1-0), whose optical depth is usually much smaller than that of HCN(1-0), to derive the column density of its main isotope HCN. The conversion from

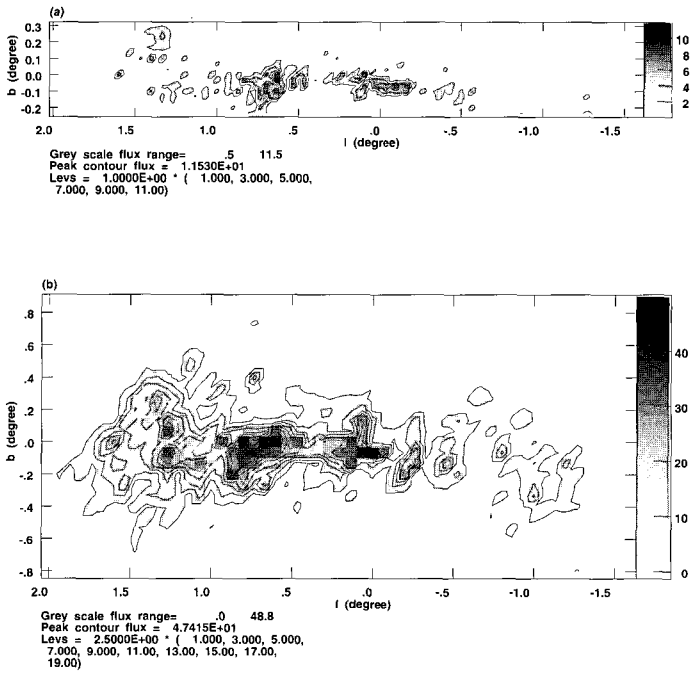

Fig. 2.— Total velocity integrated intensity maps (a) for $H^{13}CN$ J=1-0 and (b) for $H^{12}CN$ J=1-0 line. Integrated Intensities in the maps are $\int T_A^* dv/\delta v$ where δv is channel width (3.47 km s^{-1}). It is shown that the distribution of $H^{13}CN$ is very similar to that of strongly emitting cores of $H^{12}CN$ J=1-0 line, except that the $H^{13}CN$ map shows more clumpy structures than that the $H^{12}CN$ map. Emission distribution lopsided at the positive longitude is similar to that of the $H^{12}CN$ emission cores.

$N(H^{13}CN)$ to $N(H^{12}CN)$ is usually done by assuming that the conversion ratio is identical to $^{12}C/^{13}C$ ratio. The $^{12}C/^{13}C$ is one of the most frequently measured isotope ratios which ranges from about 20 to 40 in the GC region, and is known to be generally consistent with a single value of around 28 (Wannier 1989). We adopt this value as the ratio of $H^{12}CN/H^{13}CN$.

We derive $N(H^{13}CN)$ using the same formula, but with several different constants as equation (1). However, equation (2) is not applicable to derive T_{ex} of HCN(1-0) directly because the optical depth of $H^{12}CN$(1-0) is not as large as that of CO(1-0). We simply assumed that $T_{ex} = 20$ K based on the results by Cummins *et al.* (1986). Cummins *et al.* have found that T_{rot}s for many molecules in the Sgr B2 lie between about 10 and 30 K with no correlation between T_{rot} and dipole moment.

With these assumptions we derive total $H^{13}CN$ column densities of $9.2 \times 10^{13} \sim 8.0 \times 10^{14} cm^{-2}$ and infer $H^{12}CN$ column densities of $1.5 \times 10^{14} \sim 6.4 \times 10^{15} cm^{-2}$ from the ratio (=28) of $^{12}C/^{13}C$ (Table 3). Since $H^{13}CN$ line is much weaker than $H^{12}CN$ line, only core regions of $H^{12}CN$ clouds are detected with $H^{13}CN$. Thus $H^{12}CN$ column densities of the regions not detected by the $H^{13}CN$ line were derived under the assumption that the $H^{12}CN$ line is optically thin. We found these values also lie within the range of column densities mentioned above.

iii) Abundance of $H^{13}CN$

From the column densities of the H_2 and $H^{13}CN$, fractional abundance of $H^{13}CN$ relative to H_2 is obtained (Table 3). The estimated fractional abundance of $H^{13}CN$ to H_2 lies between $5.4 \times 10^{-10} \sim 2.4 \times 10^{-9}$.

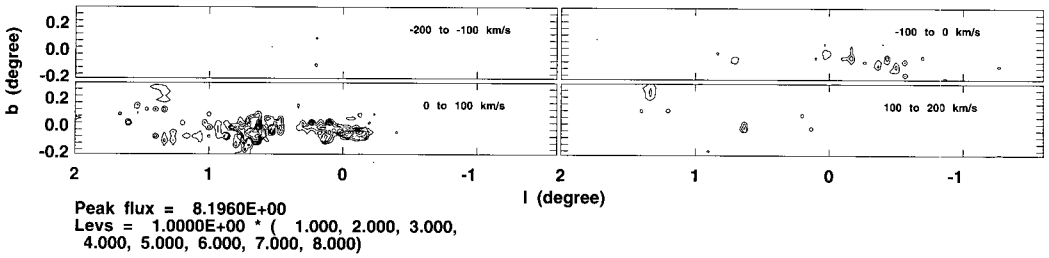

Fig. 3.— Velocity channel maps binned into 100 km s^{-1} intervals. Integrated Intensity in this map is $\int T_A^* dv/\delta v$.

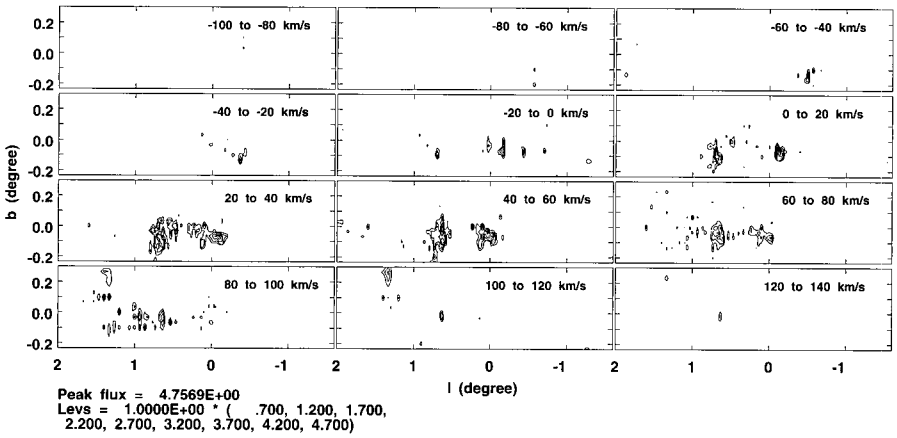

Fig. 4.— Velocity channel maps binned into 20 km s^{-1} intervals. Integrated Intensity in this map is $\int T_A^* dv/\delta v$ where δv is channel width (3.47 km s^{-1}). The scale of the Galactic latitude b is stretched a factor of two for viewing convenience.

This value is significantly higher than the value of 5.1×10^{-11} for the core of star forming molecular cloud Banard 5 by Fuller *et al.* (1991), and the value of 5.1×10^{-11} for the dark cloud L134N by Swade (1989). It is interesting that this fractional abundance is even higher than those 1.0×10^{-10} and 5.0×10^{-10} (Irvine & Schloerb 1984, and Irvine *et al.* 1987) for TMC-1 which contains unusually large abundance of carbon-bearing molecules. Fig. 7 shows some variance along with Galactic longitude within the range of $0° \leq l \leq 2°$. Obvious thing is that there is a big abundance variation at the region nearer to the GC and each value of the abundance is indeed higher than that at other cloud complexes far from the GC.

On the other hand the abundance gets constant as the clouds are farther away from the GC. This confirms that there is a rich chemistry ongoing in the near GC (e.g., Lee, Minh, & Irvine 1993).

iv) Abundance of $H^{12}CN$

The above range of $H^{13}CN$ abundance gives that of the $H^{12}CN$ abundance between 1.5×10^{-8} and 6.7×10^{-8}, by scaling with the adopted ratio of $H^{12}CN/H^{13}CN$ of 28.

Fractional abundances of $H^{12}CN$ molecules in the GC region deserve further investigation. As the $H^{13}CN$ does, the HCN abundance of GC region is also found to be highly enhanced by one order of magnitude, compared to those for Orion KL Extended Ridge (5×10^{-9}) (Blake *et al.* 1987) and L134N (2×10^{-9}) (Swade 1987) in the cold and quiescent environments. However, the HCN abundance for most regions in the GC is comparable to that (2×10^{-8}) of the cold dark cloud TMC-1 (Irvine *et al.* 1987). The HCN abundance of GC re-

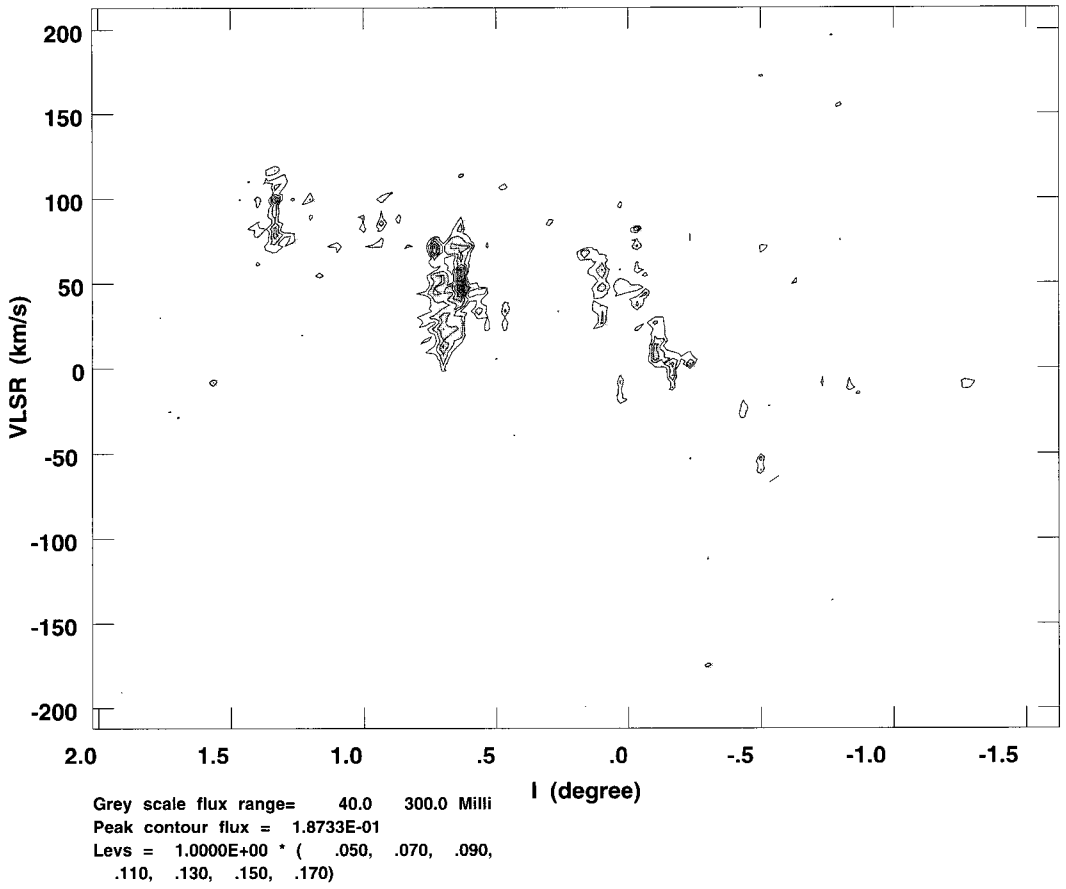

Fig. 5.— $l - V$ diagram averaged over b.

gion is smaller than those for Plateau (2.8×10^{-7}) and Hot Core (3.0×10^{-7}) of OMC-1 where extraordinary environments of shock waves and mass outflows exist due to the effect of the vicinal Luminous object IRc2 (Irvine *et al.* 1987). Fig. 8 shows more clear trend that many clouds have the various fractional abundance of HCN near the GC while the clouds far from the GC tend to have lower but uniform value. This may mean that actively energetic environment in the GC region affects the chemistry of the clouds there.

(b) Masses of Molecular Clouds

The calculation of the fractional abundance of HCN isotopes makes it possible to estimate the mass of GC clouds. Here we introduce the mass estimation of the HCN molecular clouds in the GC shown in paper 1. The mass of molecular clouds can be estimated by a summation of the mass of each pixel obtained from multiplying the pixel area ($4' \times 4'$) by the column density of the pixel $\mathrm{N(H^{12}CN)}_i$ and dividing by $\mathrm{H^{12}CN}$ fractional abundance X of the pixel;

$$Mass \approx \sum_i 1.56 \times 10^{-18} \frac{\mathrm{N(H^{12}CN)}_i}{X} \ \mathrm{M_\odot}, \qquad (4)$$

where we adopted the solar distance to the GC as 8.5 kpc.

We use the $\mathrm{H^{12}CN}$ abundance as obtained in the previous section. In other words we use $\mathrm{H^{12}CN}$ abundance inferred from $\mathrm{H^{13}CN}$ abundance in the regions where $\mathrm{H^{13}CN}$ line is detected. But in the other regions where $\mathrm{H^{13}CN}$ line is not detected, we use $\mathrm{H^{12}CN}$ abundance as derived with optically thin approximation. We assumed the abundance simply to be constant near the position where the abundance is derived. In this way we estimate the total mass of the GC molecular clouds of $\sim 2.0 \times 10^7\,\mathrm{M_\odot}$.

Previous estimates of the GC clouds range from a few $10^7 \sim 10^8\,\mathrm{M_\odot}$ (e.g., Güsten 1989; Dahmen et al. 1998; Tsuboi et al. 1999). Our mass estimate corresponds to the lower end value of the previous estimates

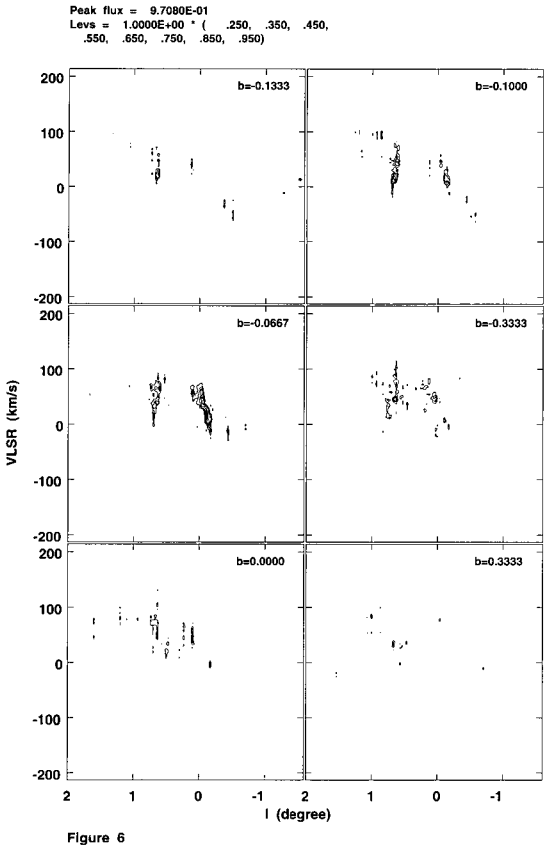

Fig. 6.— $l - V$ diagrams at several latitude b.

partly because other ones are based on mainly CO observations and CS which usually trace wider regions of the GC clouds than HCN.

We expect the uncertainty of our mass estimation is not so large. From our assumption of uncertain T_{ex} the estimation can be changed by a factor of 0.5 if the T_{ex} ranges from 10 K to 30 K. There might be a slight underestimation in the mass calculation due to the optically thin approximation of $H^{12}CN$ line at the position where $H^{13}CN$ was not detected. But such calculations were made only for the relatively small ($\sim 10^6\,M_\odot$) complexes other than the heaviest complex - the Galactic nuclear disk complex ($\sim 10^7\,M_\odot$). From such approximation the total mass should be underestimated by a factor of less than one, N($H^{12}CN$) derived under its optically thin assumption.

(c) Physical Quantities of Four Main Complexes in the GC Region

We now report estimated physical quantities (abundance of HCN isotopes, mass, and FWHM of HCN main isotope) and some characteristics of four distinct complexes in the GC, $l \approx 5.5°$ complex, $l \approx 3.2°$ complex (Bania's Clump 2), Galactic nuclear disk complex (within $-2° \leq l \leq 2°$), and $l \approx -5.5°$ complex (Bania's Clump 1). We compare these quantities each other to discuss their physical differences. The FWHM was obtained from Gaussian fit of separated components in the HCN J=1-0 profiles. Histograms of the FWHM distributions of each complexes are given in Fig. 9.

i) $l \approx 5.5°$ Complex

This complex was mapped first with $H^{12}CN$ 88.6 GHz line in paper 1 and subsequently also observed with $H^{13}CN$ 86.3 GHz line, but the latter line was not detected. The range of the $H^{12}CN$ data cube (l, b, v) of the complex was found to be between $(5°, -0.7°, 0$ km $s^{-1})$ and $(6°, 0.2°, 150$ km $s^{-1})$. Most of the spectra detected over these regions have FWHM of $\Delta V \approx 5 \sim 35$ km s^{-1} with a mode at 15 km s^{-1}, which is as broad as that of spectra in $l \approx -5.5°$ complex ($\Delta V \approx 15 \sim 35$ km s^{-1}), but less broad than those of other complexes

Table 3. COLUMN DENSITIES [cm^{-2}] AND FRACTIONAL ABUNDANCES OF HCN ISOTOPES IN THE GALACTIC CENTER REGION

$(l°, b°)$	$N(H^{12}CN)$	$N(H^{13}CN)$	$N(H_2)$	$\frac{N(H^{12}CN)}{N(H_2)}$	$\frac{N(H^{13}CN)}{N(H_2)}$
(5.4667,-0.2667)	6.0×10^{15}		2.1×10^{22}	2.9×10^{-8}	
(3.2667,0.4000)	1.0×10^{15}		5.4×10^{22}	2.2×10^{-8}	
(2.8667,0.0667)	1.2×10^{15}		4.9×10^{22}	2.5×10^{-8}	
(1.2667,-0.0667)	2.6×10^{15}	9.2×10^{13}	1.1×10^{23}	2.4×10^{-8}	8.6×10^{-10}
(0.6667,-0.0667)	5.3×10^{15}	1.9×10^{14}	2.4×10^{23}	2.2×10^{-8}	7.8×10^{-10}
(0.5333,-0.0667)	4.8×10^{15}	1.7×10^{14}	9.7×10^{22}	4.9×10^{-8}	1.8×10^{-9}
(0.4667,-0.0667)	4.7×10^{15}	1.7×10^{14}	9.1×10^{22}	5.1×10^{-8}	1.9×10^{-9}
(0.2667,-0.0667)	3.1×10^{15}	1.1×10^{14}	1.3×10^{23}	2.4×10^{-8}	8.7×10^{-10}
(0.2000,-0.0667)	3.6×10^{15}	1.3×10^{14}	1.4×10^{23}	2.6×10^{-8}	9.3×10^{-10}
(0.1333,-0.0667)	5.0×10^{15}	1.8×10^{14}	3.3×10^{23}	1.5×10^{-8}	5.5×10^{-10}
(0.0667,-0.0667)	6.4×10^{15}	2.3×10^{14}	4.2×10^{23}	1.5×10^{-8}	5.4×10^{-10}
(0.0000,-0.0667)	2.2×10^{16}	8.0×10^{14}	5.4×10^{23}	4.1×10^{-8}	1.5×10^{-9}
(-0.0667,-0.0667)	1.4×10^{16}	5.1×10^{14}	2.1×10^{23}	6.7×10^{-8}	2.4×10^{-9}
(-5.4000,0.3333)	1.5×10^{14}		9.0×10^{21}	1.7×10^{-8}	

REFERENCES.— $N(H^{13}CN)$ was estimated by LTE method under the assumption that the $H^{13}CN$ line is the optically thin. Most of $N(H^{12}CN)$ was inferred from the determined $H^{13}CN$ by scaling with the adopted ratio of $H^{12}CN/H^{13}CN$ of 28. In the positions that $H^{13}CN$ was not detected, the $N(H^{12}CN)$ was derived by assuming that the $H^{12}CN$ (1-0) line is optically thin.

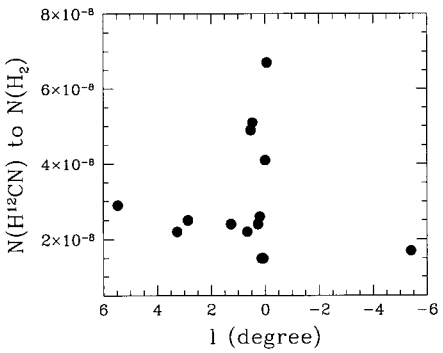

Fig. 7.— Fractional abundances of $H^{13}CN$ to H_2 in the Galactic Center region.

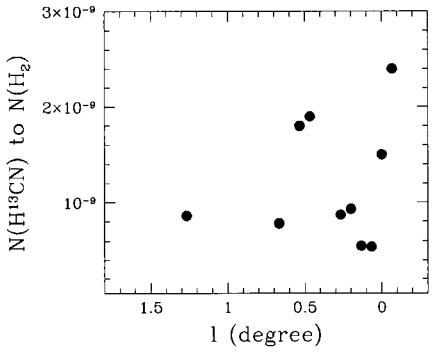

Fig. 8.— Fractional abundances of $H^{12}CN$ to H_2 in the Galactic Center region.

(Fig. 9).

The velocity structure of the complex is relatively simple. The complex contains mostly velocity components of $V_{LSR} \approx 30 \sim 150$ km s^{-1} permitted by Galactic rotation. There is no forbidden velocity components in the complex. The fractional abundance of $H^{12}CN$ at the strongly emitting region of the complex was estimated to be 2.9×10^{-8}. Assuming constancy of this abundance within the complex, the total mass of $l \approx 5.5°$ complex was found to be $\sim 1.7 \times 10^6 M_\odot$.

ii) $l \approx 3.2°$ complex

Since $l \approx 3.2$ complex, so-called Bania's Clump 2, has been known fromthe earlier CO surveys of the Galactic plane by Bania (1977), it has been studied frequently (Stark & Bania 1986, Bally *et al.* 1988, Boyce & Cohen 1989, Zylka *et al.* 1992) using a variety of molecule (^{12}CO, ^{13}CO, CS, H_2CO) lines. In the $H^{12}CN$ survey, the range of the data cube (l, b, v) of the complex was from $(2.5°, -0.4°, -20$ km $s^{-1})$ to

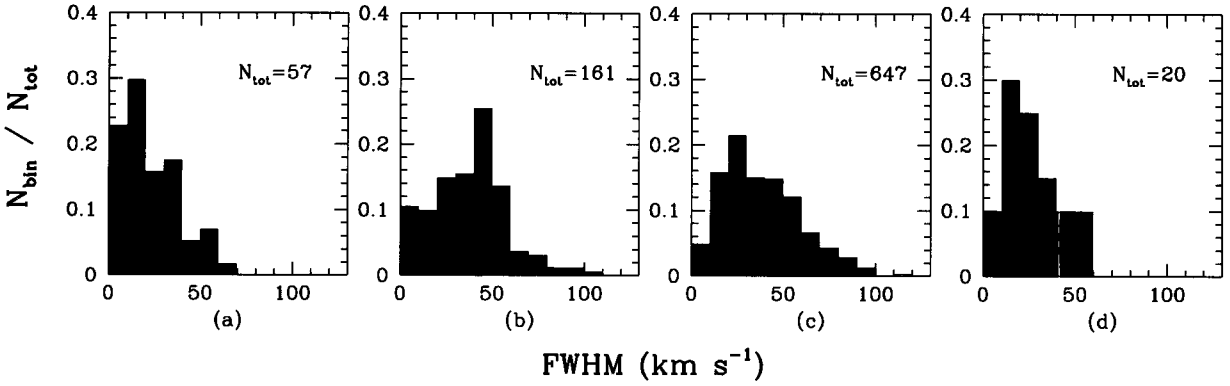

Fig. 9.— Histograms of FWHM distribution of (a) $l \approx 5.5°$ complex, (b) $l \approx 3.2°$ complex (Bania's Clump 2), (c) Galactic nuclear disk complex within $-2° \leq l \leq 2°$, and (d) $l \approx -5.5°$ complex (Bania's Clump 1). The largest mode (45 km s^{-1}) of the FWHM distributions among the complexes is in the Clump 2 . The value of the mode tends to be smaller at the farther complexes from the GC

$(4°, 0.8°, 200$ km s$^{-1})$. The H^{13}CN line was not detected. One of outstanding characteristics of the complex is the line width ($\Delta V = 25 \sim 55$ km s^{-1}) with a mode at 45 km s^{-1} as wide as that of the Galactic nuclear disk complex. Moreover there is fairly many components with $\Delta V \geq 60$ km s^{-1}, which may be due to a superposition to the line of sight of clouds in different orbits made by a barred potential in the GC (e.g., Lee *et al.* 1999).

But the kinematics of the complex is very simple compared with that of the Galactic nuclear disk complex. This complex contains mostly positive velocity components (of wide velocity range of about 200 km s^{-1}) permitted by Galactic rotation and also a few forbidden negative velocity components.

The H^{12}CN abundance of the complex is found to be between $2.0 \sim 2.5 \times 10^{-8}$. The total mass of the complex was calculated to be $\sim 3.3 \times 10^6$ M$_\odot$ assuming the fractional abundance of 2.3×10^{-8} of HCN molecules.

iii) Galactic Nuclear Disk Complex

This complex within $-2° \leq l \leq 2°$ is representative of GC clouds and includes the strongest emission regions such as Sgr A and Sgr B. This region was most extensively observed with HCN isotope lines, ^{12}CO, and ^{13}CO lines. The HCN rare isotope maps given in Fig. 2 show that this complex consists of numerous clumps which show very complex kinematics. Therefore morphology of the complex is quite different in velocity channel maps due to the systematic motions of the complex to the GC. One noticeable feature of the distribution of these clouds is the variation of the projected thickness of the emitting clouds along the Galactic longitude. The complex has a maximum projected thickness of $\sim 1.2°$ at $l \approx 1.5°$. As the longitude decreases, the projected thickness of complex decreases with a minimum size of $\sim 0.4°$ at $l \approx -0.2°$. Again the thickness of the complex increases to $l \approx -1.2°$ at which the GC complex has the second maximum projected size of $\sim 0.8°$. A likely explanation of this structure of the GC complex is that most of clouds are confined to a narrow bar or dust lane (Bally *et al.* 1988). The clouds are divided into sub-complexes of $l = 1.6°$ complex, Sgr D, Sgr A, Sgr C, and Sgr E. It is interesting that brightest emission in HCN 88.6 GHz line is at Sgr A region although Sgr B has broader bright regions than Sgr A. This contrasts with the fact that Sgr B is known to be the brightest in the sky in many molecular lines; in the case of H^{13}CN line, the Sgr B is the brightest.

The clumps in the complex have mostly FWHMs of 15$\sim$55 km s^{-1} with a mode at 25 km s^{-1}. It is noted that like the Clump 2 there are fairly many components with $\Delta V \geq 60$ km s^{-1}. The H^{12}CN abundance of the complex along the Galactic longitude at $b = -4'$ ranges from 1.5×10^{-9} to 6.7×10^{-8}. Using these abundances the total mass of the complex was calculated to be $\sim 1.4 \times 10^7$ M$_\odot$, which corresponds to about 90% of total mass of all molecular clouds within our survey area.

iv) $l \approx -5.5°$ complex (Bania's Clump 1)

The striking $l \approx -5.5°$ complex, so-called Bania's Clump 1, is known to consist of the largest non-circular velocity components of any Galactic molecular clouds from many molecular line observations (^{12}CO; Bania 1977, 1980, 1986: ^{12}CO, ^{13}CO; Bania *et al.* 1986: H_2CO; Caswell & Haynes 1982: OH; Cohen & Dent 1983: ^{13}CO; Bally *et al.* 1987, 1988). In H^{12}CN observation this complex was weakly seen relative to other complexes. Thus line profiles are not discernible with 68 km s^{-1}, 85 km s^{-1}, and 100 km s^{-1} components which were known in ^{12}CO, ^{13}CO observations of Bania *et al.* (1986). The H^{13}CN line over the complex was not detected. This complex is distributed over $(l, b) = (-4.4°, 0.1°) \sim (-5.8°, 0.7°)$.

Most clumps have fairly broad FWHMs of 15~35 km s^{-1} except for a clump in the domain of ($-5.33°, 0.45°$,-30~ -10 km s^{-1}) which has narrow FWHM of ~9 km s^{-1}. It is surprising that although they are more than ~ 900 pc away from the dynamical center of the Galaxy on the side of negative longitude, most clumps except for clump ($-4.4°, 0.55°, -60 \sim -40$ km s^{-1}) and clump ($-5.33°, 0.45°, -30 \sim -10$ km s^{-1}) have positive velocity of $V_{LSR} \approx 30 \sim 130$ km s^{-1}. This extremely forbidden velocity components can be made due to gravitational scattering of barred potential in the GC (e.g., Lee et al. 1999).

The H^{12}CN abundance at $(l, b) = (-5.4000°, 0.3333°)$ of the complex is estimated to be 1.7×10^{-8}. The total mass of the complex was calculated to be $\sim 4.9 \times 10^5\,M_\odot$ assuming this abundance over the complex.

V. SUMMARY

This paper presents results of the survey of molecular clouds toward the GC region with the H^{13}CN J=1−0 line. Most of H^{13}CN emissions are found to trace very similar distribution and velocity structures to those of the emissions of the main HCN isotope line.

The H^{13}CN line tends to be detected in the bright part among multi-components of H^{12}CN line profiles. The weak "forbidden" components in the H^{12}CN line is seldom detected in the H^{13}CN line.

We found the H^{13}CN map has an advantage to look at more details of the velocity structures of the saturated regions of the HCN clouds with better contrast. This enables us to calculate velocity gradients at Sgr A and B (about 2.1 and 5.2 km s^{-1} pc^{-1}, respectively) which are found to be very large, comparing with that (~ 0.7 km s^{-1} pc^{-1}) inferred from the Galactic rotation within ~ 350 pc.

We estimated physical quantities such as fractional abundance of HCN isotopes, mass, and FWHM of the molecular clouds in the GC to study the characteristics of the clouds, using the H^{12}CN (J=1-0), H^{13}CN (J=1-0), ^{12}CO (J=1-0) and ^{13}CO (J=1-0) line data.

The fractional abundance of H^{13}CN to H_2 was between $5.4 \times 10^{-10} \sim 2.4 \times 10^{-9}$. The H^{12}CN abundance was inferred to be between 1.5×10^{-8} and 6.7×10^{-8}, by scaling with the adopted ratio of H^{12}CN/H^{13}CN of 28. These abundances in the GC clouds were found to be highly enhanced by one order of magnitude, compared to those in the cold and quiescent clouds. There are some trends that the clouds near the GC have the various fractional abundance of HCN with highly enhanced value and the clouds distant from the GC have relatively lower but uniform abundance.

Our total mass estimate of the HCN molecular clouds within $|l| \leq 6°$ was found to be $\sim 2 \times 10^7\,M_\odot$ using HCN isotope abundance. Most of mass is in the Galactic nuclear disk complex ($\sim 1.4 \times 10^7\,M_\odot$).

The largest mode (45 km s^{-1}) of the FWHM distributions among the complexes is in the Clump 2 and the mode tends to be smaller as a complex is located farther from the GC.

ACKNOWLEDGEMENTS

This research is supported in part by grant KOSEF R01-2003-000-10513-0 from the Basic Research Program of the Korea Science and Engineering Foundation, and in part by Strategic National R&D Program (M1-0222-00-0005) from Ministry of Science and Technology, Republic of Korea.

REFERENCES

Bally, J., Stark, A. A., Wilson, R. W., & Henkel, C. 1987, Galactic center molecular clouds. I - Spatial and spatial-velocity maps, ApJ, 65, 13.

Bally, J., Stark, A. A., Wilson, R. W., & Henkel, C. 1988, Galactic center molecular clouds. II - Distribution and kinematics, ApJ, 324, 223

Bania, T. M. 1977, Carbon monoxide in the inner Galaxy, ApJ, 216, 381

Bania, T. M. 1980, Carbon monoxide in the inner Galaxy - tHE 3 KIloparsec arm and other expanding features, ApJ, 242, 95

Bania, T. M. 1986, A latitude survey of carbon monoxide emission near the Galactic center, ApJ, 307, 350

Bania, T. M., Stark, A. A. & Heiligman G. M. 1986, Clump 1 - an unusual molecular cloud complex near the Galactic center, ApJ, 308, 868

Blake, G. A., Sutton, E. C., Masson, C. R., & Phillips, T. G. 1987, Molecular abundances in OMC-1 - The chemical composition of interstellar molecular clouds and the influence of massive star formation, ApJ, 315, 621

Boyce, P. J., Cohen, R. J. 1989, *The Center Of The Galaxy*, IAU Symp. No. 136, Dordrecht : Kluwer, P. 141.

Caswell, J. L., & Haynes, R. F. 1982, High-velocity H II regions delineating a central bar in our Galaxy, ApJL, 254, L31

Cohen, R. J. & Dent,W. R. F. 1983, *Surveys of the Southern Galaxy*, ed. W. B. Burton & F. P. Israel (Dordrecht : Reidel), p.159

Cummins, S. E., & Thaddeus, P., & Linke, R. A. 1986, A survey of the millimeter-wave spectrum of Sagittarius B2, ApJS, 60, 819

Dahmen, G., Huttemeister, S., Wilson, T. L., & Mauersberger, R. 1998, Molecular gas in the Galactic center region. II. Gas mass and $N_{H_2}/I_{^{12}CO}$ conversion based on a $C^{18}O(J = 1 \rightarrow 0)$ survey, A&A, 331, 959

Dickman, R. L. 1978, The ratio of carbon monoxide to molecular hydrogen in interstellar dark clouds, ApJS, 37, 407

Fuller, G.A., Myers, P. C., Goldsmith, P. F., Langer, W. D., & Campbell B. G. 1991, Anatomy of the Barnard 5 core, ApJ, 376, 135

Gordon, M. A., & Burton, W. B. 1976, Carbon monoxide in the Galaxy. I - The radial distribution of CO, H_2, and nucleons, ApJ, 208, 346

Güsten, R. 1989, *The Center Of The Galaxy*, IAU Symp. No. 136, Dordrecht : Kluwer, P. 89

Heiligman, G. M. 1987, Molecular gas within 2 deg of the Galactic center. I - Survey of ^{13}CO emission, ApJ, 314, 747

Irvine, W. M., Goldsmith, P. F.& Hjalmarson, Å. 1987, *Interstellar Process*, eds. D. J. Hollenbach, H. A. Thronson, Jr., P. 561

Irvine, W. M., & Schloerb, F. P. 1984, Cyanide and isocyanide abundances in the cold, dark cloud TMC-1, ApJ, 282, 516

Lee, C. W., Minh, Y. C., & Irvine, W.M. 1993, Observations of C_3H_2 (2_{12} - 1_{01}) Toward the Sagittarius A Molecular Cloud, JKAS, 26, 73

Lee, C. W. 1996, Dense Molecular Clouds in the Galactic Center Region. I. HCN (J = 1–0) Data, ApJS, 105, 129 (paper 1)

Lee, C. W., Lee, H. M., Ann, H. B., & Kwon, K. H. 1999, Smoothed Particle Hydrodynamic Simulations of Galactic Gaseous Disk with Bar: Distribution and Kinematic Structure of Molecular Clouds toward the Galactic Center, ApJ, 513, 242

Minh, Y. C., Irvine, W. M., & Friberg, P. 1992, Molecular abundances in the Sagittarius A molecular cloud, A&A, 258, 489

Miyazaki, A. & Tsuboi, M. 2000, Dense Molecular Clouds in the Galactic Center Region. II. Statistical Properties of the Galactic Center Molecular Clouds, ApJ, 536, 357

Morris, M., & Serabyn, E. The Galactic Center Environment, 1996, ARAA, 34, 645

Oka, T., Hasegawa, T., Sato, F., Tsuboi, M., Miyazaki, A., Sugimoto, M. 2001, Statistical Properties of Molecular Clouds in the Galactic Center, ApJ, 562, 34.

Oka, T., Hasegawa, T., Sato, F., Tsuboi, & M., Miyazaki, A. 1998, A Large-Scale CO Survey of the Galactic Center, ApJS, 118, 455

Park, Y. S., Han, S. T., Park, J. A., & Kim, H. R. 1994, Efficiencies of Daeduk Radio Telescope in 40 - 150 GH range, TRAO Technical Report No. 10

Stark, A. A., Bally, J., Knapp, G. R., & Wilson, R. W. 1988, *Molecular Clouds in the Milky Way and in External Galaxies*, Heidelberg : Springer-Verlag, New York, P. 303

Stark, A. A. & Bania, T. M. 1986, Clump 2 - an inner spiral arm?, ApJ, 306, L17

Swade, D. A. 1989, The physics and chemistry of the L134N molecular core, ApJ, 345, 828

Swade, D. A. 1987, Ph.D Dissertation, University of Massachusetts

Tsuboi, M., Handa, T., & Ukita, M. 1999, Dense Molecular Clouds in the Galactic Center Region. I. Observations and Data, ApJS, 120, 1

Wannier, P. G. 1989, *The Center Of The Galaxy*, IAU Symp. No. **136**, Dordrecht : Kluwer, P. 107

Zylka, R., Güsten, R., Henkel, C. & Batrla, W. 1992, H_2CO survey in the galactic center - L = 0.5-4.0 deg, A&AS, 96, 525